Int. J. of Applied Mechanics and Engineering, 2016, vol.21, No.2, pp.485-510
DOI: 10.1515/ijame-2016-0029

PROBABILISTIC BUCKLING ANALYSIS OF THE BEAM STEEL STRUCTURES SUBJECTED TO FIRE BY THE STOCHASTIC FINITE ELEMENT METHOD

P. ŚWITA
Department of Civil Engineering and Environmental Engineering
Faculty of Technical Sciences, State University of Applied Sciences
35 kard. S. Wyszyński Str., 62-510 Konin, POLAND
E-mail: piotr.swita@konin.edu.pl

M. KAMIŃSKI*
Department of Structural Mechanics, Faculty of Civil Engineering,
Architecture and Environmental Engineering, Łódź University of Technology
Al. Politechniki 6, 90-924 Łódź, POLAND
E-mail: marcin.kaminski@p.lodz.pl
Department of Civil Engineering and Environmental Engineering
Faculty of Technical Sciences, State University of Applied Sciences
35 kard. S. Wyszyński Str., 62-510 Konin, POLAND

The main purpose is to present the stochastic perturbation-based Finite Element Method analysis of the stability in the issues related to the influence of high temperature resulting from a fire directly connected with the reliability analysis of such structures. The thin-walled beam structures with constant cross-sectional thickness are uploaded with typical constant loads, variable loads and, additionally, a temperature increase and we look for the first critical value equivalent to the global stability loss. Such an analysis is carried out in the probabilistic context to determine as precisely as possible the safety margins according to the civil engineering Eurocode statements. To achieve this goal we employ the additional design-oriented Finite Element Method program and computer algebra system to get the analytical polynomial functions relating the critical pressure (or force) and several random design parameters; all the models are state-dependent as we consider an additional reduction of the strength parameters due to the temperature increase. The first four probabilistic moments of the critical forces are computed assuming that the input random parameters have all Gaussian probability functions truncated to the positive values only. Finally, the reliability index is calculated according to the First Order Reliability Method (FORM) by an application of the limit function as a difference in-between critical pressure and maximum compression stress determined in the given structures to verify their durability according to the demands of EU engineering designing codes related to the fire situation.

Key words: stability analysis, linearized buckling, fire simulation, stochastic perturbation method, stochastic finite element method, response function method, reliability analysis.

1. Introduction

Probabilistic analysis of the structures (Elishakoff [1], Kamiński [2]) includes still many unresolved problems, especially when related to the steel structures area (Waarts and Vrouwelvender [3]). Modern and recent applications deal with the castellated steel beams (Ellobody [4]), stiffened panels (Graham and Siragy [5]) or structural elements subjected to a corrosion process (Sadovský and Drdàcký [6]). The other works were more focused on computational methods and issues, where geometrical imperfections of the uncertain

* To whom correspondence should be addressed

nature are included (Papadopoulos *et al*. [7]). Also, the very interesting and challenging problems of the post-buckling paths were analyzed (Steinböck *et al*. [8]). However, determination of the higher probabilistic moments of both structural response and buckling modes is still very rare and the classical Monte-Carlo simulation is preferred. This is especially important in the area of thermo-elastic problems with temperature-dependent material coefficients and practically important in many coupled problems like fire accidents, where a temperature may be higher than thousand degrees within the first few minutes of fire ignition. The very rapid fluctuations of the temperature, which practically is unpredictable, may lead to almost a complete loss of the structural steel strength and elasticity. Such a practical analysis deserves a detailed computer analysis, especially with the technique preserving the efficiency of the Monte-Carlo simulation but consuming definitely less time.

The main goal of numerical analyze contained in this paper is to determine the parameters of random critical force steel structures with a random temperature using the stochastic perturbation method and compare the results with the results of the Monte-Carlo simulation (Kamiński [2]; Kalos and Whitlock [9]). As it was experimentally verified all the structural elements are highly sensitive to the fire and the same is true for their stability limits. Such an analysis will allow the design of fire safety of steel elements especially in terms of their reliability (Eurocode 3 [10]). In the analysis of the behavior of structures in fire temperatures the ultimate limit state, which is understood as the exhaustion of portability charges by item or excessive deformation of the structure. Exhaustion of the slender construction of the load may lead to the loss of stability due to the strength reduction of the basic parameters. The essence of the issues is the random behavior of the structure under higher temperature, where the temperature contributes to the determination of random variables as strength parameters. It should be noted that numerical simulation of a real fire is complex due to the fact that a temperature, which is for sure mostly uncertain, induces automatically the entire set of random mechanical and physical parameters influencing dramatically all the structural state parameters. This analysis is an attempt to connect the structure stability issues with the operation of the higher temperature for the reliability assessment of stochastic structures. In the analysis of elastic stability the Stochastic Finite Element Method (SFEM) (Kleiber and Hien [11]; Kamiński [2]) combined with the Response Function Method are used. First the polynomial response functions in-between the Young modulus connected with higher temperature and a critical force are found through the series with FEM experiments with a varying design parameter value. A computer system is totally responsible for the Least Squares Method approximation of these analytical functions. The results of the stochastic perturbation method were compared with the results of alternative techniques such as the Monte-Carlo simulation. The generalized stochastic perturbation technique employed here in its tenth order version to calculate expected values, coefficients of variation, skewness and kurtosis of the critical pressure with respect to the input coefficient of variation fluctuations to verify whether the Gaussian character of the random input is preserved in the linearized buckling problem (Elishakoff [12]).

Additionally, we take into account the fact that mechanical properties of the steel are significantly reduced together with a temperature increase due to the fire. Some experimentally driven functions are adopted after the recommended civil engineering design codes here (and also numerically smoothed throughout the discrete values via the Least Squares Method with higher order splines). One may recover from our analyses the time fluctuations of the basic probabilistic characteristics of the critical force after an application of the so-called fire curves that describe temperature variations in time during such a normative fire. Therefore, in fact random Gaussian input temperature induces non-stationary stochastic process of the buckling resistivity of the given structures (Øksendal [13]). We assume some steady-state distribution of the temperature inside the element or the structure for the brevity of further presentation and discussion, but a more realistic approach would be to analyze a coupled thermal-mechanical problem with transient heat transfer accounting for temperature-dependent steel parameters and some additional uncertainty source(s). Our methodology is illustrated by using two examples – a simple column entirely subjected to the fire and a part of the building, where the fire scenarios include partial heating of the given floor. Both tests show that a critical temperature for both deterministic and stochastic case study belongs to the interval $\theta \in \left[500°C, 600°C\right]$. It results in exceeding the limit states in the deterministic analysis, while the stochastic approach shows big discrepancies in probabilistic characteristics of the critical forces and too small values of

the reliability index. The practical engineering importance of this study is emphasized by the fact that the existing Eurocodes do not include any guide to the determination of the reliability index in case of stability limits as well as in case of fire accidents (and also their protection and prevention).

2. The stochastic perturbation method in stability and reliability analysis

The random variable b is considered and also its probability density function $p_b(x)$. The main objective of the stochastic perturbation method is to develop all the input random variables as well as all the state functions in a Taylor series about their mean values using the perturbation parameter ε. The random critical force may be rewritten in the presence of such an uncertainty as Kamiński and Świta [14]

$$P_{cr} = P_{cr}^{0} + \sum_{n=1}^{\infty} \frac{1}{n!} \varepsilon^n \frac{\partial^n P_{cr}}{\partial b^n} (\Delta b)^n \tag{2.1}$$

where

$$\varepsilon \Delta b = \varepsilon \left(b - b^0 \right), \tag{2.2}$$

is the first variation of b around its expected value b^0 and

$$\varepsilon^2 (\Delta b)^2 = \varepsilon^2 \left(b - b^0 \right)^2, \tag{2.3}$$

is the second order variation of b. The expected value of the critical force can be defined as

$$E\left[P_{cr}(b) \right] = \int_{-\infty}^{+\infty} P_{cr}(b) p_b(x) dx = \int_{-\infty}^{+\infty} \left(P_{cr}^{0} + \sum_{n=1}^{\infty} \frac{1}{n!} \varepsilon^n \frac{\partial^n P_{cr}}{\partial b^n} \Delta b^n \right) p_b(x) dx. \tag{2.4}$$

This development is true if and only if the series converges and this unconditional convergence is guaranteed by an application of the polynomial representation of the critical forces in addition to the given input random parameter. All the convergence criteria must include the parameter ε, which a priori is assumed to be equal to 1 in engineering calculations. Numerical examples presented further in this work demonstrate an impact of the expected values, standard deviations and other characteristics of random approaches of different orders of the proposed perturbation methodology.

From the numerical point of view, the development shown in formula (2.1) is written as an infinite sum, however Eq.(2.4) as an integral one is always determined for the real finite limits, where the lower and also the upper limit of this integration procedure must have a physical justification and are frequently determined in an experimental way. Independently from the particular form of the desired probability function, the expected value for a symmetric distribution function can be derived according to the following formula

$$E\left[P_{cr}(b) \right] = P_{cr}^{0} + \int_{-\infty}^{+\infty} \left(\sum_{n=1}^{2N} \frac{1}{(2n)!} \varepsilon^{2n} \frac{\partial^{2n} P_{cr}}{\partial b^{2n}} \Delta b^{2n} \right) p_b(x) dx, \quad n \in N. \tag{2.5}$$

One may expand and integrate the above to get

$$E\left[P_{cr}(b)\right]=P_{cr}\left(b^0\right)+\frac{1}{2}\varepsilon^2\frac{\partial^2 P_{cr}\left(b^0\right)}{\partial b^2}\mu_2\left(b^0\right)+\ldots+\frac{1}{2m!}\varepsilon^m\frac{\partial^{2m}P_{cr}\left(b^0\right)}{\partial b^{2m}}\mu_{2m}\left(b^0\right), \quad (2.6)$$

and

$$\mu_{2m+1}=0, \qquad \mu_{2m}=1\cdot 3\cdot\ldots\cdot(2m-1)\sigma^{2m}, \qquad \text{for} \quad m=1,2,3,\ldots., \quad (2.7)$$

where σ denotes standard deviation of the random parameter *b*. Generally, the *m*th central probabilistic moment of the critical force is defined as

$$\mu_{\mathrm{m}}\left(P_{cr}(b)\right)=\int_{-\infty}^{+\infty}\left(P_{cr}\left(b^0\right)-\mathrm{E}\left[P_{cr}\left(b^0\right)\right]\right)^m p_b(x)\,dx. \quad (2.8)$$

This formula renders it possible to derive a perturbation-based relation describing a variance of the critical force $P_{cr}(b)$ in terms of the Gaussian random input *b*. It can be written as

$$\mu_2\left(P_{cr}(b)\right)=\mathrm{var}\left(P_{cr}(b)\right)=\int_{-\infty}^{+\infty}\left(P_{cr}\left(b^0\right)-E\left[P_{cr}\left(b^0\right)\right]\right)^2 p_b(x)\,dx. \quad (2.9)$$

Given the above assumptions, the variance is derived now according to the twelfth order approximation that includes automatically all lower order expansions of the second, fourth, sixth, eighth and also the tenth order. For the twelfth order approximation of the variance of the critical force there holds

$$\begin{aligned}
\mathrm{Var}\left(P_{cr}(b)\right)=&\varepsilon^2\mu_2(b)\left(D_{[1]}\left(P_{cr}\right)\right)^2+\varepsilon^4\mu_4(b)\left(\frac{1}{4}\left(D_{[2]}\left(P_{cr}\right)\right)^2+\frac{2}{3!}D_{[1]}\left(P_{cr}\right)D_{[3]}\left(P_{cr}\right)\right)+\\
&+\varepsilon^6\mu_6(b)\left(\left(\frac{1}{3!}\right)^2\left(D_{[3]}\left(P_{cr}\right)\right)^2+\frac{1}{4!}D_{[2,4]}\left(P_{cr}\right)+\frac{2}{5!}D_{[1,5]}\left(P_{cr}\right)\right)+\\
&+\varepsilon^8\mu_8(b)\left(\frac{1}{6!}D_{[2,6]}\left(P_{cr}\right)+\frac{2}{7!}D_{[1,7]}\left(P_{cr}\right)+\frac{70}{8!}\left(D_{[4]}\left(P_{cr}\right)\right)^2+\frac{2}{6!}D_{[3,5]}\left(P_{cr}\right)\right)+\\
&+\varepsilon^{10}\mu_{10}(b)\left(\frac{252}{10!}\left(D_{[5]}\left(P_{cr}\right)\right)^2+\frac{42}{9!}D_{[4,6]}\left(P_{cr}\right)+\frac{1}{8!}D_{[2,8]}\left(P_{cr}\right)+\frac{24}{9!}D_{[3,7]}\left(P_{cr}\right)+\right.\\
&\left.+\frac{2}{9!}D_{[1,9]}\left(P_{cr}\right)\right)+\varepsilon^{12}\mu_{12}(b)\left(\frac{2}{11!}D_{[1,11]}\left(P_{cr}\right)+\frac{1}{10!}D_{[2,10]}\left(P_{cr}\right)+\frac{440}{12!}D_{[3,9]}\left(P_{cr}\right)+\right.\\
&\left.+\frac{7}{10!}\left(D_{[6]}\left(P_{cr}\right)\right)^2+\frac{990}{12!}D_{[4,8]}\left(P_{cr}\right)+\frac{12}{10!}D_{[5,7]}\left(P_{cr}\right)\right)
\end{aligned} \quad (2.10)$$

where $D_{[i]}(P_{cr})$ and $D_{[i,j]}(P_{cr})$ denote the *i*th derivatives and also a product of *i*th and *j*th derivatives of the critical force in addition to the random parameter *b*. All higher order statistics may be derived additionally by using of Eq.(2.8) in conjunction with an expansion provided by Eq.(2.1) and have been developed in the tenth order version for other than stability problems in Kamiński [2].

Computational implementation of the symbolic calculus programs combined with the visualization of probabilistic output moments ensures most probably the fastest solution of such a problem. Thanks to such a series representation of the random output, any desired efficiency of the expected values as well as higher probabilistic moments can be achieved by an appropriate choice of the expansion length (and some additional correction available in the parameter ε) which generally depends on the input probability density function (PDF) type, interrelations between the probabilistic moments, acceptable error of the computations, etc. These congruent derivations lead to higher order expansions and equations for third and fourth central probabilistic moments necessary for a determination of the skewness and kurtosis of the given output variable (Kamiński [2]). Having determined the first two probabilistic moments of the critical force one may calculate the reliability index using the limit function *g* according to the following formula (Cornell [15])

$$\beta = \frac{E[g]}{\sigma(g)} = \frac{E[P_{cr} - Q]}{\sigma(P_{cr} - Q)} = \frac{E[P_{cr}] - E[Q]}{\sqrt{Var(P_{cr} - Q)}} = \frac{E[P_{cr}] - E[Q]}{\sqrt{Var(P_{cr}) + Var(Q)}} \tag{2.11}$$

where P_{cr} denotes the additional structural capacity, while Q stands for the extreme structural response.

The probability of survival P_f is to be found from the following relation:

$$P_f = \Phi(-\beta) \tag{2.12}$$

where Φ is a probability density function of the standardized Gaussian distribution. Quite naturally, we assume that the critical force and the extreme value of the compressive force are statistically independent from each other (this second force is usually treated even as a deterministic quantity), so that the cross-correlation in the denominator of Eq.(2.11) is frequently postponed; additionally, this extreme compressive force does not depend upon the fire temperature in our tests. One needs to realize that the value of the parameter ε is traditionally introduced in all derivations with this perturbation technique as equal to 1 (Kleiber and Hien [11]).

3. Elastic stability by the combined Stochastic Finite Elements and the Response Function Method

The purpose to use the tenth order Stochastic Finite Element Method in conjunction with the Response Function Method is the necessity to determine higher order partial derivatives of the critical forces in addition to the given random input parameter. Lower order versions of the SFEM (Kleiber and Hien [11]) were released with the use of hierarchical equations, whose numerical matrix solution led to a straightforward determination of the increasing orders perturbation terms contributing to the equations for the overall probabilistic moments.

The Finite Element Method (FEM) discretization (Bathe [16]; Zienkiewicz and Taylor [17]) is connected here with the Response Function Method (RFM) convenient for a further solution of the structural stability problem exhibiting uncertainty in parameters related to the temperature. The sequences of the deterministic solutions were performed, where the input random parameter value is treated as deterministically varying around its mean value – for the brevity of presentation the new index α is used here to expose this variability. Then, the global stability equation can be formulated as Kamiński and Świta [18]

$$\left(\boldsymbol{K}_{(\alpha)}^{(s)}(\theta) + \lambda_{(\alpha)}(\theta)\,\boldsymbol{K}_{(\alpha)}^{(\sigma)}\left(\hat{F}_{(\alpha)};\theta\right)\right)\boldsymbol{r}_{(\alpha)}(\theta) = \lambda_{(\alpha)}(\theta)\,\hat{\boldsymbol{R}}_{(\alpha)}(\theta) \tag{3.1}$$

where $\boldsymbol{K}_{(\alpha)}^{(\sigma)}\left(\hat{F}_{(\alpha)};\theta\right)$ is the series of geometric stiffness matrix calculated independently for each discrete temperature θ, $\boldsymbol{K}_{(\alpha)}^{(s)}(\theta)$ is the series of the elastic stiffness matrix determined in the same way, the loading

temperature dependent series are denoted here by $\boldsymbol{R}_{(\alpha)}(\theta)$. When some structural element is subjected to the temperature fluctuation $\Delta\theta$ we have to deal with its initial deformation $\varepsilon_O = \alpha_T(\Delta\theta)$, where α_T is the thermal expansion coefficient of steel. Therefore, the loading series can be expressed as

$$\boldsymbol{R}_{(\alpha)}(\theta) = \boldsymbol{P}_{(\alpha)}(\theta) + \boldsymbol{Q}_{(\alpha)}(\theta) \tag{3.2}$$

where $\boldsymbol{P}_{(\alpha)}(\theta)$ is the external load vector and $\boldsymbol{Q}_{(\alpha)}(\theta)$ is the load applied in the nodes of the element resulting from the actual mesh deformation. It is known that the series $\boldsymbol{R}_{(\alpha)}(\theta)$ have all proportional character to $\lambda_{(\alpha)}(\theta)\hat{\boldsymbol{R}}_{(\alpha)}(\theta)$ where $\lambda_{(\alpha)}(\theta)$ stand for the loading factor series and $\hat{\boldsymbol{R}}_{(\alpha)}(\theta)$ is some loading. Further, the distribution of internal forces $\hat{\boldsymbol{F}}_{(\alpha)}(\theta)$ is equivalent to the load $\hat{\boldsymbol{R}}_{(\alpha)}(\theta)$ and the displacement $\boldsymbol{r}_{(\alpha)}(\theta)$ is equivalent to the load $\lambda_{(\alpha)}(\theta)\hat{\boldsymbol{R}}_{(\alpha)}(\theta)$. Therefore, we determine the values of $\lambda_{(\alpha)}(\theta)$ from the following dual condition

$$\begin{cases} \left(\boldsymbol{K}^{(s)}_{(\alpha)}(\theta) + \lambda_{(\alpha)}(\theta)\boldsymbol{K}^{(\sigma)}_{(\alpha)}\left(\hat{F}_{(\alpha)};\theta\right)\right)\boldsymbol{r}_{1(\alpha)}(\theta) = \lambda_{(\alpha)}(\theta)\hat{\boldsymbol{R}}_{(\alpha)}(\theta) \\ \left(\boldsymbol{K}^{(s)}_{(\alpha)}(\theta) + \lambda_{(\alpha)}(\theta)\boldsymbol{K}^{(\sigma)}_{(\alpha)}\left(\hat{F}_{(\alpha)};\theta\right)\right)\boldsymbol{r}_{2(\alpha)}(\theta) = \lambda_{(\alpha)}(\theta)\hat{\boldsymbol{R}}_{(\alpha)}(\theta) \end{cases}, \boldsymbol{r}_{1(\alpha)}(\theta) - \boldsymbol{r}_{2(\alpha)}(\theta) = \boldsymbol{v}_{(\alpha)}(\theta), \tag{3.3}$$

so that we obtain the basic algebraic equation series representing the temperature-dependent elastic stability

$$\left(\boldsymbol{K}^{(s)}_{(\alpha)}(\theta) + \lambda_{(\alpha)}(\theta)\boldsymbol{K}^{(\sigma)}_{(\alpha)}\left(\hat{F}_{(\alpha)};\theta\right)\right)\boldsymbol{v}_{(\alpha)}(\theta) = 0. \tag{3.4}$$

Therefore, the basic condition that one can get for the critical value at the given temperature $\lambda_{(\alpha)} = \lambda_{cr(\alpha)}(\theta)$ and for critical load $\boldsymbol{R}_{cr(\alpha)}(\theta) = \lambda_{cr(\alpha)}(\theta)\hat{\boldsymbol{R}}_{(\alpha)}(\theta)$ is the following one

$$\det\left(\boldsymbol{K}^{(s)}_{(\alpha)}(\theta) + \lambda_{(\alpha)}(\theta)\boldsymbol{K}^{(\sigma)}_{(\alpha)}\left(\hat{F}_{(\alpha)};\theta\right)\right) = 0. \tag{3.5}$$

The critical force is represented in simple structural case studies as

$$P_{cr}(\theta) = \lambda_{cr}(\theta)\hat{R}(\theta). \tag{3.6}$$

According to the basic idea of the Response Function Method we adopt some polynomial representations of the critical values $\lambda_{cr}(\theta)$ with respect to the input random variable b as

$$\lambda_{cr}(\theta) = \sum_{k=0}^{n} D_k(\theta) b^k. \tag{3.7}$$

The coefficients $D_k(\theta)$ are determined numerically from several deterministic solutions to the original stability matrix equation with the random parameter value fluctuating about its mean value in the interval $b = \left[b^0 - \Delta b, b^0 + \Delta b\right]$ at different temperatures. The nonlinear non-weighted least square fitting

technique implemented in the computer algebra system MAPLE is employed for this purpose. The Response Function Method involves the following minimization

$$\min \sum_{i=1}^{N}\left(\lambda_{cr(i)}(\theta)-\sum_{k=0}^{n} D_k(\theta) b_{(i)}^{k}\right)^2 = \min \sum_{i=1}^{N} e_i^2(\theta), \tag{3.8}$$

and

$$S\left(D_k(\theta)\right) = \sum_{i=1}^{N} e_i^2(\theta). \tag{3.9}$$

Of course, all partial derivatives inherent in the expression (3.9) with respect to the coefficients D_i are set to be equal to zero. Finally, the critical values random derivatives are calculated analytically with the use of the following recursive formula

$$\frac{\partial^k \lambda_{cr}(\theta)}{\partial b^k} = \prod_{j=1}^{k}(n-j) D_1(\theta) b^{n-k} + \prod_{j=2}^{k}(n-j) D_2(\theta) b^{n-(k+1)} + \ldots + D_{n-k}(\theta) \tag{3.10}$$

where the most frequent differentiation with respect to the random temperature looks like

$$\frac{\partial^k \lambda_{cr}(\theta)}{\partial \theta^k} = \frac{\partial^k \lambda_{cr}(\theta)}{\partial E^k(\theta)} \frac{\partial^k E(\theta)}{\partial \theta^k}. \tag{3.11}$$

4. Computational experiments

4.1. Compression of the simply supported bar under uniform fire heating

The first analysis concerns the steel beam shown in Fig.1. A model of the column consists of a rod with a length of *14.0 m* manufactured with the use of the hot-rolled steel profile HEB300. This profile belongs to the first class according to the steel structures designing rules, which is equivalent to the slenderness larger than its limit value. The static scheme is equivalent to the single straight element compressed axially on its both sides. The load in a form of the compressive force *650 kN* is applied to the supported node and the temperature of the rod is gradually increased. All further calculations have been performed using the presented version of the perturbation method and compared with the results obtained using the relevant statistical estimators obtained from the Monte-Carlo simulation; statistical estimation is carried out by applying of the traditional estimators presented in Bendat and Piersol [19]. Deterministic stability analysis has been performed here using the computer program *Autodesk Robot Structural Analysis 2012* based on the Finite Element Method, for a discretization consisting of 999 elastic bar two-noded finite elements. Quite naturally, the temperature of this element has been chosen as the Gaussian input random variable with the given expectation varying in the temperatures interval given in Tab.1, while its coefficient of variation is the next additional parameter into our computational analysis.

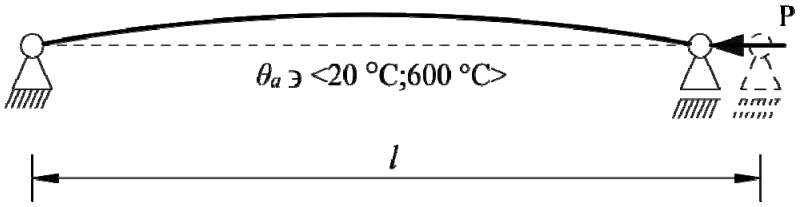

Fig.1. Static scheme of the heated element.

Assuming that the rate of heating of the steel is in the range of *20-50 K/min* and using relations contained in the engineering design codes, these reduction factors are defined as follows

$$f_{p,\theta} = k_{p,\theta}\ f_y, \quad f_{y,\theta} = k_{y,\theta}\ f_y, \quad E_{a,\theta} = k_{E,\theta}\ E. \tag{4.1}$$

The coefficients $k_{p,\theta}$, $k_{y,\theta}$, $k_{E,\theta}$ are each the measures of the relative reduction in mechanical properties due to heating by a fire. These reduction factors, the critical values and critical forces are summarized in Tab.1.

Tab.1. Reduction factors for the stress-strain curves of carbon steels at elevated temperatures and the critical load value of the first deformation as a function of the temperature.

Steel temperature	Reduction factors at temperature Θ_a relative to the value of f_y or E_a at 20^oC			Random elasticity modulus $E_{a\Theta}$	The critical value for first buckling form λ_{cr}	The critical force for first buckling form $P_{cr}(\Theta)$
	Reduction factor (relative to f_y) for effective field strength	Reduction factor (relative to f_y) for proportional limit	Reduction factor (relative to E_a) for the slope of the linear elastic range			
1	2	3	4	5	6	7
Θ_a	$k_{y,\theta} = f_{y,\theta}/f_y$	$k_{p,\theta} = f_{p,\theta}/f_y$	$k_{E,\theta} = E_{a,\theta}/E$	$\left[\frac{N}{mm^2}\right]$	$\lambda_{cr} = \frac{P_{cr}(\Theta)}{P}$	$[kN]$
20°C	*1.000*	*1.000*	*1.000*	*210000*	*4.10*	*2661.62*
100°C	*1.000*	*1.000*	*1.000*	*210000*	*4.10*	*2661.62*
200°C	*1.000*	*0.807*	***0.900***	***189000***	***3.69***	***2395.46***
300°C	*1.000*	*0.613*	***0.800***	***168000***	***3.28***	***2129.30***
400°C	*1.000*	*0.420*	***0.700***	***147000***	***2.87***	***1863.13***
500°C	*0.780*	*0.360*	***0.600***	***126000***	***2.46***	***1596.97***
600°C	*0.470*	*0.180*	***0.310***	***65100***	***1.27***	***825.10***
700°C	*0.230*	*0.075*	*0.130*	*27300*	*0.46*	*300.38*

Table 1 documents that the fire entirely heating any structural element decreases the linear elastic modulus E_a in higher temperatures decisively faster than the yield stress. It means that the serviceability limit state is more sensitive to a fire accident than the Ultimate Limit State. Therefore, the temperature just above $\Theta=100^oC$ decreases the critical value related to the structural buckling. Reduction in yield strength, even though it has a more violent nature, occurs only above $\Theta=400^oC$. All the calculations have been performed sequentially with temperature increments $\Theta=100^oC$ with a corresponding reduction in the modulus of elasticity according to the values collected in Tab.1. We have carried out stability analysis for the temperatures in the interval [20^oC, 600^oC] as the critical temperature $\Theta=700^oC$ exceeds the critical force. Usage of the Response Function Method to recover the first critical force computed for various temperatures demands some polynomial basis. The best fitting is obtained as

$$P_{cr}(\Theta) = -7.687 \cdot 10^{-15} \cdot \Theta^7 + 1.507 \cdot 10^{-11} \cdot \Theta^6 - 1.162 \cdot 10^{-8} \cdot \Theta^5 + \\ + 4.406 \cdot 10^{-6} \cdot \Theta^4 - 8.186 \cdot 10^{-4} \cdot \Theta^3 + 5.632 \cdot 10^{-2} \cdot \Theta^2 + \\ - 0.832 \cdot \Theta + 2661.620 \quad [kN], \tag{4.2}$$

and is presented in Fig.2. The curve in Fig.2 coincides perfectly with the set of discrete points adjacent to several deterministic solutions (maximum deviation is *-0.00048*%). The critical values obviously decrease together with an increasing temperature, analogously to the elastic modulus thermal fluctuations.

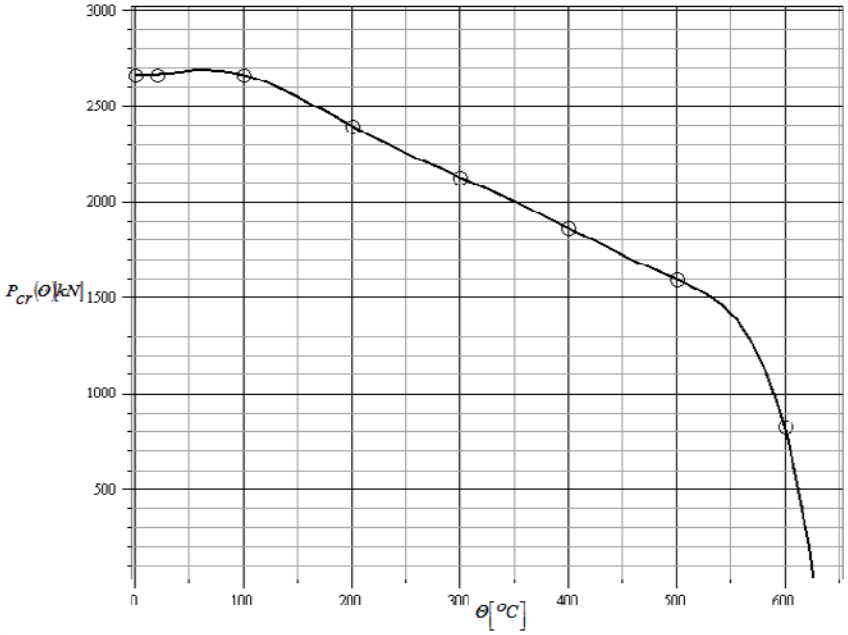

Fig.2. The response function $P_{cr} = P_{cr}(\theta)$.

In order to obtain the equations depending on a single independent variable, namely the input coefficient of variation of random temperature and to have a direct comparison with the Monte-Carlo simulation (MCS), further calculations are all based on the perturbation parameter $\varepsilon=1$. A comparison of the results obtained by the perturbation stochastic method summarizes the results of the Monte-Carlo simulation (MCS) in accordance with the normal distribution of size $n=10^5$ trials; program MAPLE has been used as the random number generator. The elastic modulus has been initially determined as a function of temperature prior to this simulation. The most optimal Least Squares Method approximation for this function can be represented as

$$E(\Theta) = -0.606 \cdot 10^{-12} \cdot \Theta^7 + 0.119 \cdot 10^{-8} \cdot \Theta^6 - 0.917 \cdot 10^{-6} \cdot \Theta^5 + \\ + 0.348 \cdot 10^{-3} \cdot \Theta^4 - 0.646 \cdot 10^{-1} \cdot \Theta^3 + 4.443 \cdot \Theta^2 + \\ - 65.670 \cdot \Theta + 210000 \quad [MPa]. \tag{4.3}$$

Probabilistic convergence tests have been provided for the very wide range of the input coefficient of variation, e.g. $\alpha \in [0.00; 0.40]$. A remarkable similarity of the variances of the critical force was obtained for $\alpha \in [0.00; 0.20]$ for the temperatures $\Theta=100^oC$ and $\Theta=200^oC$ and (Figs 3 and 4) and the twelfth order of stochastic perturbation-based results is the closest to the estimators coming from the MCS in the given temperatures range. As it could be expected, the variances of the critical force at both temperatures dominantly increase together with an increase of the input coefficient of variation and the resulting functions

are convex and generally rather close to a series of the discrete values obtained via computer simulation. This is may be not the case of lower order stochastic perturbation methods (especially of the second order), whose results should be treated as not efficient for larger input uncertainty. This observation affects also the reliability analysis and that is why the tenth order is preferred.

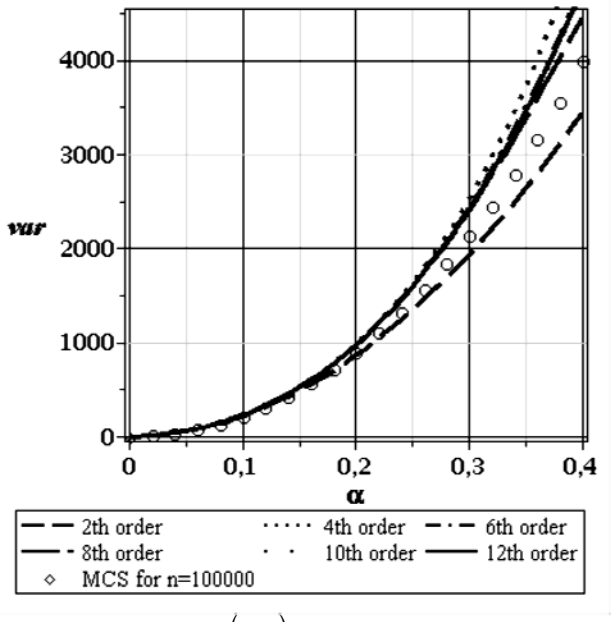

Fig.3. Variance $Var\left(P_{cr}\right)$, a comparison of the perturbation method and MCS, $\mathrm{E}\left[\Theta\right]$=*100°C*.

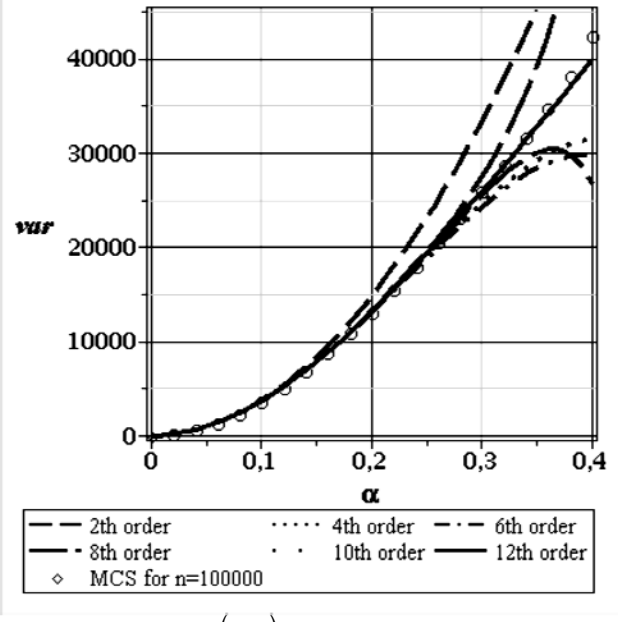

Fig.4. Variance $Var\left(P_{cr}\right)$, a comparison of the perturbation method and MCS, $\mathrm{E}\left[\Theta\right]$=*200°C*.

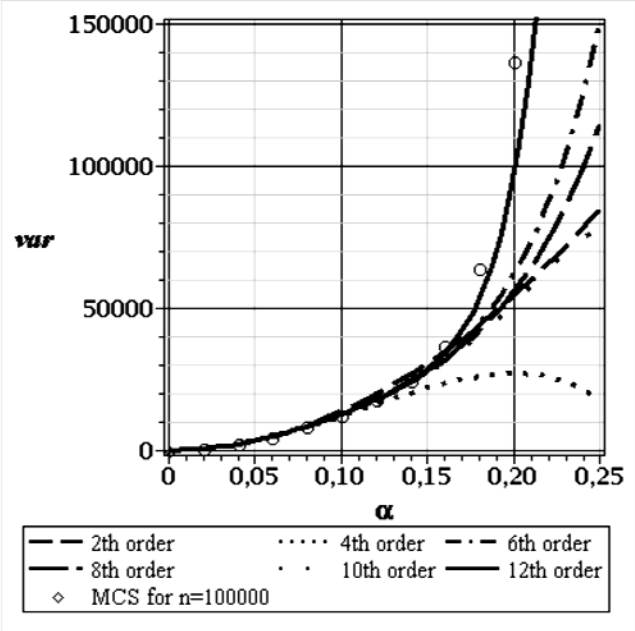

Fig.5. Variance $Var\left(P_{cr}\right)$, a comparison of the perturbation method and MCS, $\mathrm{E}\left[\Theta\right]$=*400°C*.

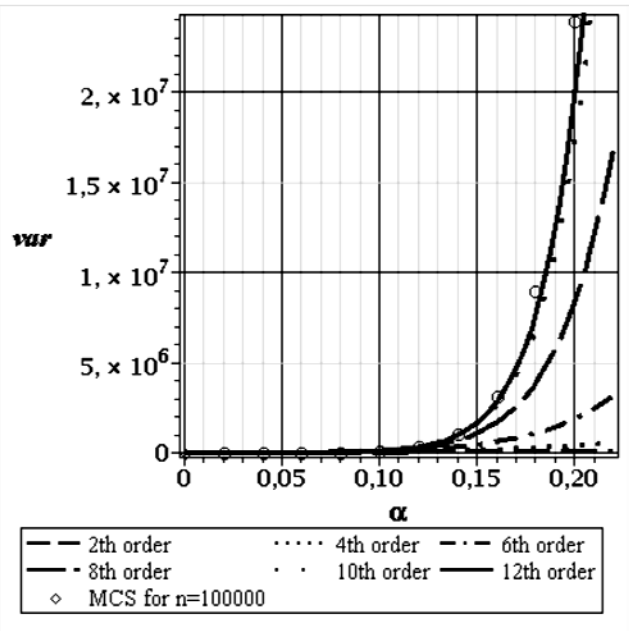

Fig.6. Variance $Var\left(P_{cr}\right)$, a comparison of the perturbation method and MCS, $\mathrm{E}\left[\Theta\right]$=*500°C*.

As it is documented by the results obtained for each temperature, the highest accuracy in-between statistical estimators of the Monte-Carlo Simulation (MCS) and the stochastic perturbation technique is

obtained for its twelfth order implementation. A distribution of various orders of the stochastic perturbation technique is the most regular for extreme temperature $\Theta=500^{o}C$. It is observed that the higher the order of the stochastic perturbation method at a specific range of the coefficient of variation, the smaller the difference in-between neighboring orders results (Fig.6). Further, an important observation concerns the distribution of the resulting critical force in the context of computed coefficient of skewness, and also the third central probabilistic moment. As we know, this parameter is equal to zero for the Gaussian probability distribution function (and for all the symmetric distributions also). Starting from the results presented in Figs 7 and 8, where skewness determined via both the stochastic perturbation method and MCS approach differs from zero we need to conclude that the given input Gaussian random variable does not induce the Gaussian critical force; it remains true for $\Theta\geq 100\,^{o}C$. This conclusion is entirely confirmed by the analysis of kurtosis (Figs 9-10) also different from zero – generally positive for most of the perturbation methods results and sometimes even negative.

An increase of the temperature and an increase in the coefficient of variation result in the divergent values of the skewness and kurtosis in-between successive perturbation order approaches, which is particularly apparent for the temperature $\Theta=500^{o}C$ and for $\alpha>0.06$ (Figs 8 and 10). A comparison of the results obtained for the stochastic perturbation methods and for the Monte-Carlo simulation reveals a good coincidence of both methods. It is interesting that a better coincidence in-between these methods is obtained for a higher temperature, while $\Theta=100^{o}C$ results in significantly more distant results. In order to obtain a better convergence of these two methods it is recommended first to increase the total number of the MCS random trials (to more than a million).

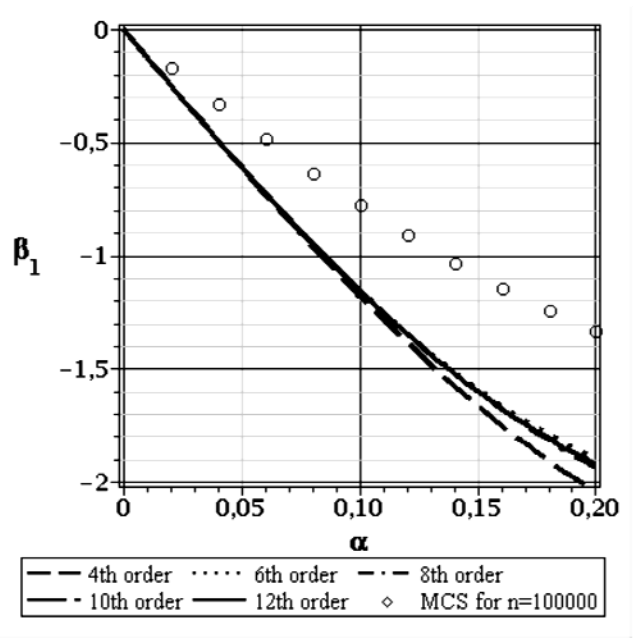

Fig.7. Skewness $\beta_1\left(P_{cr}\right)$, a comparison of the perturbation method and MCS, $\mathrm{E}\left[\Theta\right]=100^{o}C$.

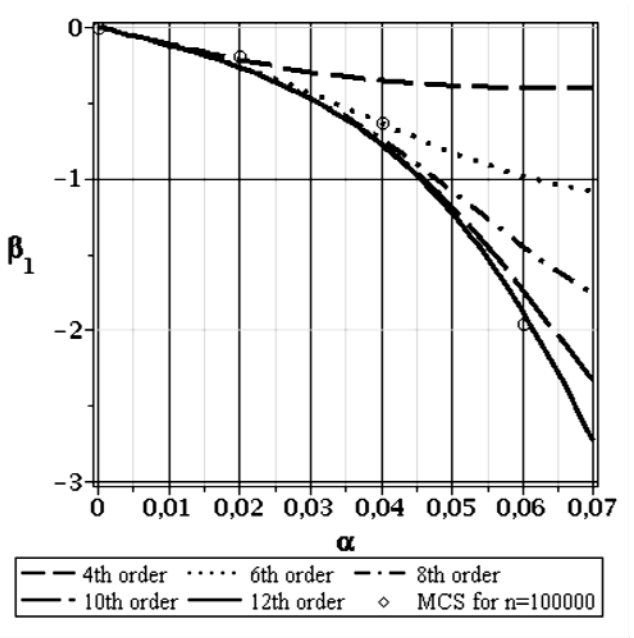

Fig.8. Skewness $\beta_1\left(P_{cr}\right)$, a comparison of the perturbation method and MCS, $\mathrm{E}\left[\Theta\right]=500^{o}C$.

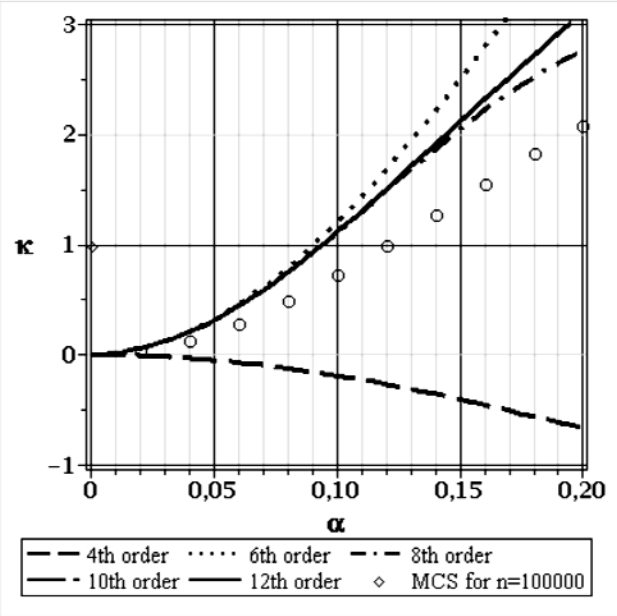

Fig.9. Kurtosis $\kappa\left(P_{cr}\right)$, a comparison of the perturbation method and MCS, $\mathrm{E}[\Theta]=100^{o}C$.

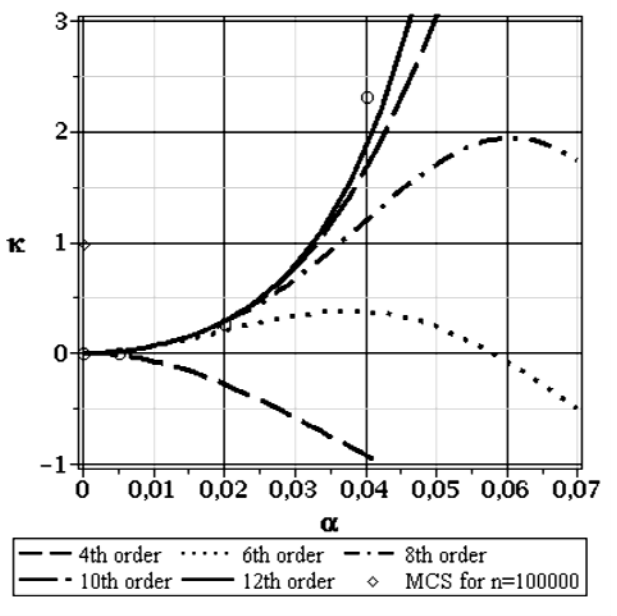

Fig.10. Kurtosis $\kappa\left(P_{cr}\right)$, a comparison of the perturbation method and MCS, $\mathrm{E}[\Theta]=500^{o}C$.

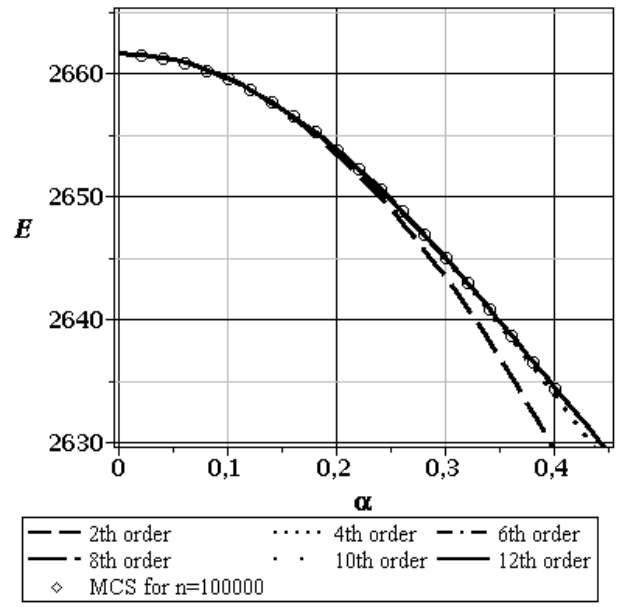

Fig.11. Expected value $E\left[P_{cr}\right]$, a comparison of the perturbation method and MCS, $\mathrm{E}[\Theta]=100^{o}C$.

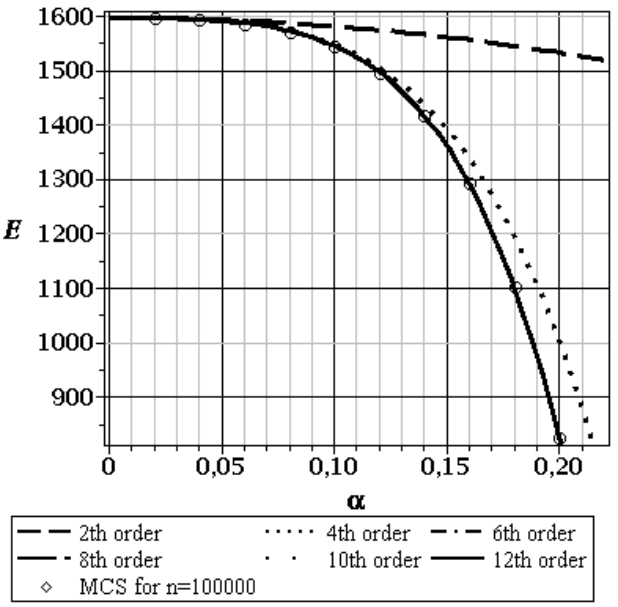

Fig.12. Expected value $E\left[P_{cr}\right]$, a comparison of the perturbation method and MCS, $\mathrm{E}[\Theta]=500^{o}C$.

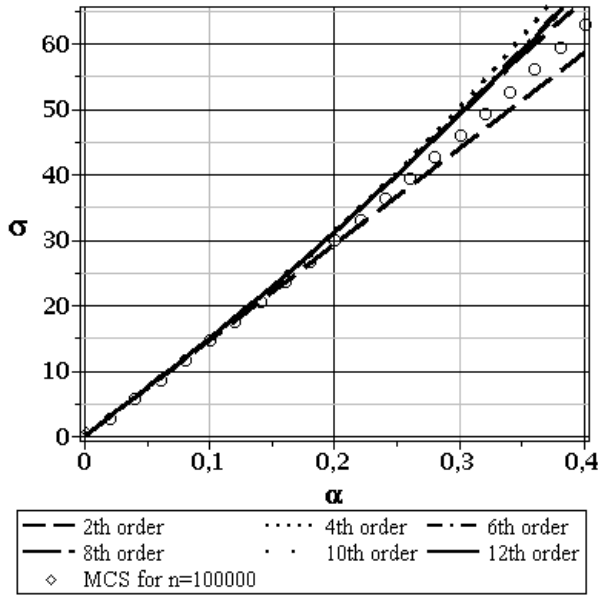

Fig.13. Standard deviation $\sigma\left(P_{cr}\right)$, a comparison of the perturbation method and MCS, $\mathrm{E}[\Theta]=100^{o}C$.

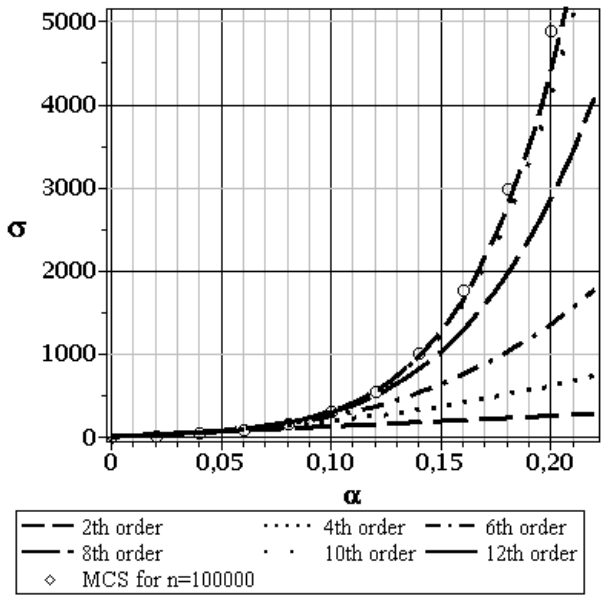

Fig.14. Standard deviation $\sigma\left(P_{cr}\right)$, a comparison of the perturbation method and MCS, $\mathrm{E}[\Theta]=500^{o}C$.

Analyzing the probabilistic convergence of the particular moments of the critical force we conclude quite obviously that the best efficiency is obtained for the expectations, where even the sixth-order perturbation technique coincide very well with the MCS estimation. Let us note that the difference of the expected value obtained by the stochastic perturbation method and, separately, with the use of MCS is generally less than *0.001*%, so that can be postponed at all. This coincidence in-between the MCS and the SPM is a little bit weaker for the standard deviation, nevertheless is quite satisfactory. Interestingly, the output standard deviation of the critical force is almost linearly dependent upon the input uncertainty $\alpha(T)$ for $\mathrm{E}[\Theta]=100^{o}C$, and it nonlinearly increases while $\mathrm{E}[\Theta]=500^{o}C$, especially above $\alpha(T)>0.10$. The differences between the results obtained for the stochastic perturbation method of various orders are decisively smaller for a lower temperature here (cf. Fig.13). Figures 11-14 document consecutively that the twelfth order perturbation technique is really very efficient in determining the expectations and standard deviations despite of the value of $\alpha(T)$. This conclusion is of the practical importance as these moments influence the reliability index only and its value fluctuations depending upon the element temperature, probabilistic numerical technique and also upon the input coefficient of variation have been collected in Tabs 2-3 below. Additionally, one may find numerical values of the expectations and variances resulting in this index for lower and higher temperatures.

Tab.2. Comparison of reliability index by MCS and by the Stochastic Perturbation Method, $\mathrm{E}\left[\Theta = 100\,^{O}C\right]$.

MONTE-CARLO SIMULATION for $n=10^5$			
α	$Var\left[P_{cr}\right]$	$E[P_{cr}]$	β
0.02	*8.58*	*2661.54*	*686.63*
0.04	*34.39*	*2661.30*	*342.98*
0.06	*77.60*	*2660.90*	*228.28*
0.08	*138.51*	*2660.35*	*170.82*
0.10	*217.51*	*2659.63*	*136.26*
0.12	*315.12*	*2658.77*	*113.16*
0.14	*431.89*	*2657.75*	*96.61*
0.16	*568.47*	*2656.60*	*84.16*
0.18	*725.52*	*2655.30*	*74.45*
0.20	*903.70*	*2653.87*	*66.66*

STOCHASTIC PERTURBATION METHOD			
α	$Var\left[P_{cr}\right]$	$E\left[P_{cr}\right]$	β
0.02	*8.59*	*2661.54*	*686.46*
0.04	*34.49*	*2661.30*	*342.50*
0.06	*78.11*	*2660.90*	*227.53*
0.08	*140.14*	*2660.34*	*169.82*
0.10	*221.50*	*2659.62*	*135.03*
0.12	*447.02*	*2658.76*	*111.71*
0.14	*594.04*	*2657.74*	*94.96*
0.16	*568.47*	*2656.58*	*82.33*
0.18	*765.99*	*2655.28*	*72.45*
0.20	*964.52*	*2653.85*	*64.52*

Tab.3. Comparison of reliability index by MCS and by the Stochastic Perturbation Method, $\mathrm{E}\left[\Theta = 500\,^{O}C\right]$.

MONTE-CARLO SIMULATION for $n=10^5$			
α	$Var\left[P_{cr}\right]$	$E[P_{cr}]$	β
0.02	*654.17*	*1596.29*	*37.00*
0.04	*3088.89*	*1593.57*	*16.98*
0.06	*9617.30*	*1586.82*	*9.55*
0.08	*29123.45*	*1572.48*	*5.41*
0.10	*94188.42*	*1545.14*	*2.92*
0.12	*314119.60*	*1497.06*	*1.51*
0.14	*1020171.00*	*1417.60*	*0.76*
0.16	*3125287.00*	*1292.49*	*0.36*
0.18	*8944484.00*	*1103.02*	*0.15*
0.20	*23940695.00*	*825.04*	*0.04*

STOCHASTIC PERTURBATION METHOD			
α	$Var\left[P_{cr}\right]$	$E[P_{cr}]$	β
0.02	*654.46*	*1596.27*	*36.99*
0.04	*3098.20*	*1593.53*	*16.95*
0.06	*9660.76*	*1586.75*	*9.53*
0.08	*28981.47*	*1572.37*	*5.42*
0.10	*90982.87*	*1544.98*	*2.97*
0.12	*289107.90*	*1496.83*	*1.58*
0.14	*884156.20*	*1417.32*	*0.82*
0.16	*2532523.00*	*1292.22*	*0.40*
0.18	*6744108.00*	*1102.88*	*0.17*
0.20	*16734729.00*	*825.29*	*0.04*

The first very important observation is that the reliability index obtained for a minimum value of $\alpha(T)=0.02$ and smaller $\mathrm{E}[\Theta]=100^{o}C$ is about twenty times larger than that close to the critical temperature, for $\mathrm{E}[\Theta]=500^{o}C$. The first two probabilistic moments computed with the use of both numerical techniques are perfectly the same in pairs – for smaller and larger temperatures, separately. It means that stability analysis with temperature uncertainty for small scale engineering structures may be carried out with the use of the stochastic perturbation method without any computational discrepancy. Interestingly, that expected value of the critical force decreases by about *60*% for the considered fire temperature fluctuation, but the variance increases by almost eighty times. Further, smaller temperature is accompanied by uncertainty-independent critical force expectation, while for $\mathrm{E}[\Theta]=500^{o}\mathrm{C}$ this expectation decreases two times over the entire random scale. The variances increase definitely faster (the only contribution to the reliability index denominator) – a hundred times at the initial temperature and almost 10^4 times for a higher temperature. It results in the fact that the final value of the reliability index decreases here in a typical exponential manner (ten times for a lower temperature throughout the entire variability range of $\alpha(T)$). Higher temperature tests exhibit a critical state of this element shortly above $\alpha(T)=0.08$, which is a relatively small uncertainty level concerning the fire temperature nature. Even in this limit case statistical and non-statistical methods give the same results, which is rather far beyond initial expectations.

4.2. Six nave frame building under non-uniform fire

The second example concerns probabilistic characteristics of a building structure subjected to high temperature caused by a fire also in the context of the global stability of the complex bar structure. The subject of our analysis is a six nave steel frame consisting of 639 bars made of the hot rolled steel profiles (Fig.15) classified as the first class sections. All the columns are made of the steel hot-rolled wide flange profiles HEB 320. The floor beams are made of the very similar profiles HEB 400, whereas the transverse beams (stiffening) were designed as HEB 260. All connections between the beams have been established for the brevity of presentation and discussion as perfectly rigid (according to the engineering designing codes their stiffness depends on the inter-connected elements actual temperature). Each rod has been subdivided here into a minimum of 32 two-noded finite elements, which gives a total of 20449 beam finite elements and 20118 nodes; three-storey columns are completely fixed in their foundations $u_x=0$, $u_z=0$, $u_y=0$. The freedom of a deformation of the entire structure has been disabled along the axis y $\left(u_y=0\right)$, which is perpendicular to the main plane of this frame (cf. Fig.15). This structure is uploaded with its dead load (No.1), static load - roof, walls and floors load (No.2) and fire temperature (No.3). In addition, a uniform constant live load is applied to the beams of each floor (No.4), static equivalent of the wind pressure (No.5) and finally snow (No.6). The global buckling coefficient has been further determined for the dominating load combination in the form of (No.1 + No.2) *1.35* + (No.3) *1.10* + (No.4) *1.05* + (No.5) *0.90* + (No.6) *0.75*.

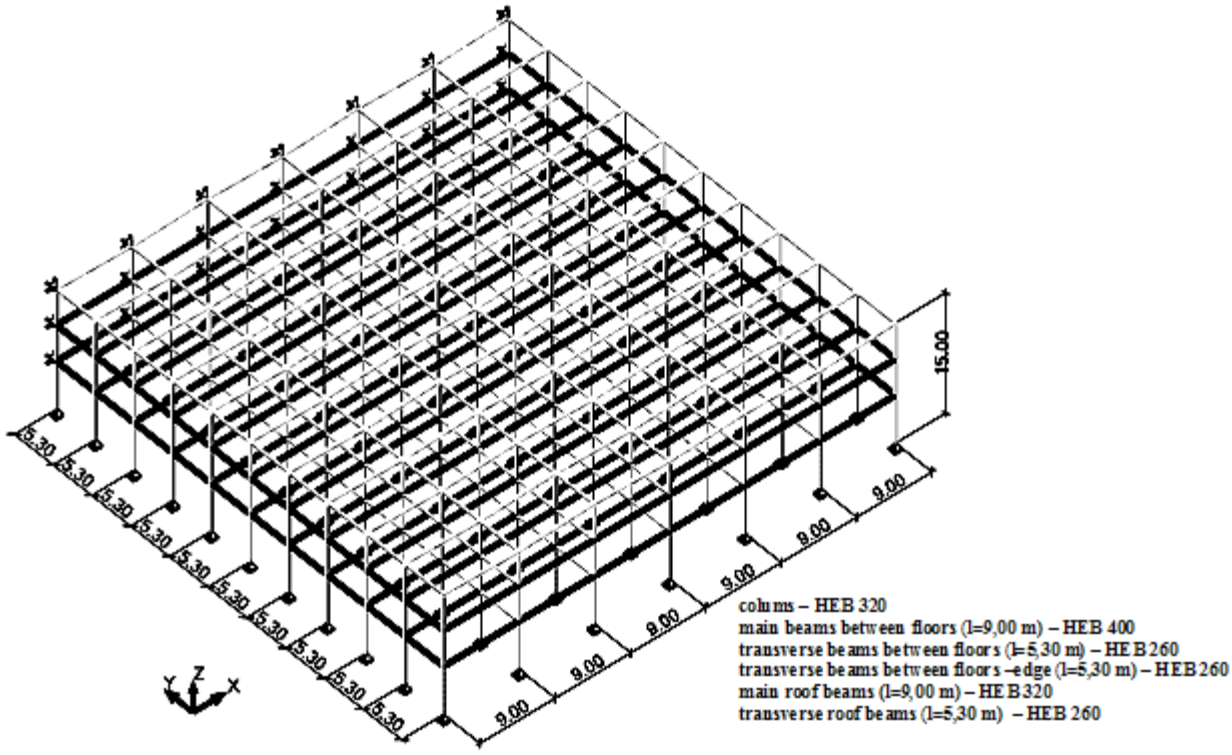

Fig.15. Static scheme of the building.

A reduction of the elasticity modulus and yield strength in higher temperatures has been made according to the experimental data included in Tab.4. The additional internal forces caused by heating the structure in the temperature range belonging to $20^{o}C \le \Theta < 750^{o}C$ are included as proposed in the engineering design codes as the relative thermal expansion of steel defined as

$$\frac{\Delta l}{l} = 1.2 \cdot 10^{-5} \cdot \Theta + 0.4 \cdot 10^{-8} \cdot \Theta^{2} - 2.416 \cdot 10^{-4} . \tag{4.4}$$

Considering the fact that the critical temperature has been initially calculated from the engineering code in a deterministic way as a little bit smaller than $\Theta = 700^{o}C$, then the temperature range for probabilistic computations has been set as [*0°C*; *680°C*]. All the reduction factors necessary for materially non-linear analysis are inserted in Tab.4. It is seen that the largest decrease of the critical force is obtained in the range *500-600°C*, where the first critical force reduces by almost *65%*, similar decisive decreases are obtained for all material parameters contained in this table.

Successively, the building is divided into fire zones (four zones dividing the building into four sectors), while at the same time the structure has been subjected to a combination of loads and uniform utilization of temperature, applied to one zone in accordance with Fig.16. These zones are thermally separated, and the structural members subjected to a higher temperature are not thermally insulated. The ceilings between the floors do not separate any fire, so that all structural elements of the given fire zone have been uniformly heated by the temperature Θ. Deterministic and probabilistic computations of the critical load for this structure model have been performed by means of the geometrically nonlinear analysis by using the Newton-Raphson algorithm. The computer FEM analysis has been performed using the *Autodesk Robot Structural Analysis 2012* program, where a number of critical forces have been determined as a function of the fire temperature. All these calculations have been carried out for the temperatures listed in Tab.4 including a corresponding reduction in the elastic modulus. The discrete sets of critical forces have been replaced for the needs of any order stochastic

perturbation method into some polynomial function of the input temperature by the Least Squares Method. The first and second deformed configurations are contrasted for the corresponding critical loads in Figs 17-18 below. The main difference between them is that the first form of buckling deformation is almost the same for all the columns (pure bending mode), while the other strongly depends upon the position of a given column inside this building (combined bending-twisting mode).

Tab.4. Reduction factors for the stress-strain curves for carbon steels at the elevated temperatures and the critical load value of the first deformation as a function of temperature.

Steel Temperature	Reduction factors at temperature Θ_a relative to the value of f_y or E_a at 20^oC			Random modulus of elasticity E_a	The critical value for first buckling form λ_{cr}	The critical force for first buckling form $P_{cr}(\Theta)$
	Reduction factor for the effective field strength	Reduction factor for the proportionality limit	Reduction factor for a slope of the linear elastic range			
1	2	3	4	5	6	7
Θ_a	$k_{y,\theta}=f_{y,\theta}/f_y$	$k_{p,\theta}=f_{p,\theta}/f_y$	$k_{E,\theta}=E_{a,\theta}/E$	$\left[\frac{N}{mm^2}\right]$	$\lambda_{cr}=\frac{P_{cr}(\Theta)}{P}$	$[kN]$
20^oC	*1.000*	*1.000*	*1.000*	*210000*	*3.765*	*4782.47*
100^oC	*1.000*	*1.000*	*1.000*	*210000*	*3.765*	*4731.50*
200^oC	*1.000*	*0.807*	*0.900*	*189000*	*3.685*	*4580.94*
300^oC	*1.000*	*0.613*	*0.800*	*168000*	*3.592*	*4427.26*
400^oC	*1.000*	*0.420*	*0.700*	*147000*	*3.483*	*4256.24*
500^oC	*0.780*	*0.360*	*0.600*	*126000*	*3.361*	*4094.93*
600^oC	*0.470*	*0.180*	*0.310*	*65100*	*2.201*	*2720.57*
650^oC	*0.350*	*0.128*	*0.220*	*46200*	*2.122*	*2619.16*
680^oC	*0.278*	*0.096*	*0.166*	*34860*	*1.269*	*1581.92*
700^oC	*0.230*	*0.075*	*0.130*	*27300*	*0.974*	*1124.85*

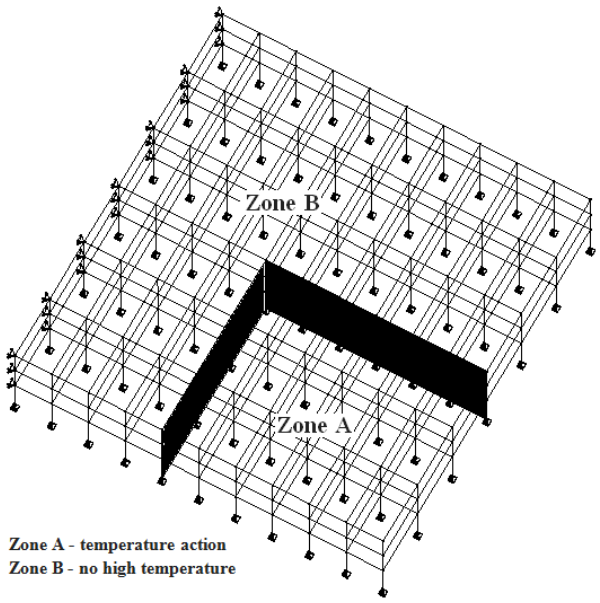

Fig.16. Diagram of temperature load equivalent to the fire accident (No.3).

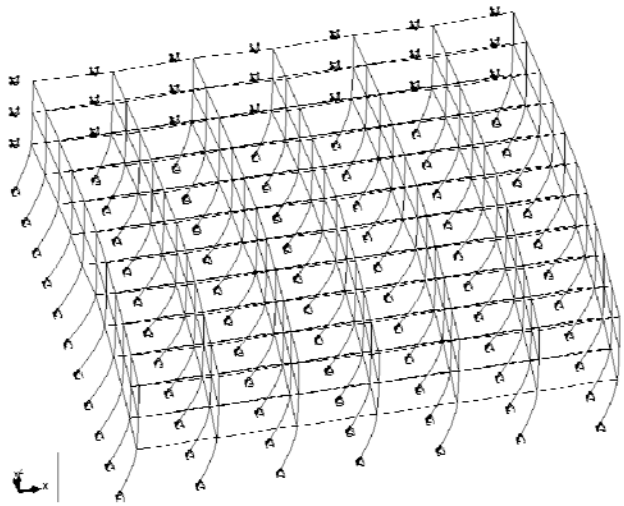

Fig.17. Structure deformation equivalent to the first critical load, $\mathrm{E}[\Theta] = 680^{o}\,C$.

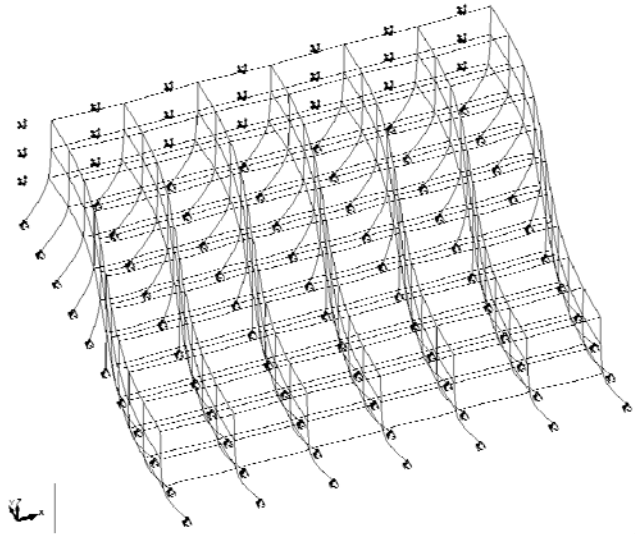

Fig.18. Structure deformation equivalent to the second critical load, $\mathrm{E}[\Theta] = 680^{o}\,C$.

Preliminary results of these computations are contained in Figs 19-20 and these are the compressive force in the most loaded column as well as the first critical force – both as a function of the mean fire temperature. These graphs contain discrete values obtained in the FEM experiments together with their continuous polynomial approximations returned by the LSM. It is very interesting that these two forces exhibit completely different temperature variations. They decrease at the same time in the range [*0°C*, *500°C*] in a very regular and monotonous way and then a compressive force starts to suddenly increase, while the critical one rapidly decreases together with an additional temperature increase. These reversed tendencies in P_{real} and P_{cr} lead to the most decisive decrease of the reliability index given further in Tab.5.

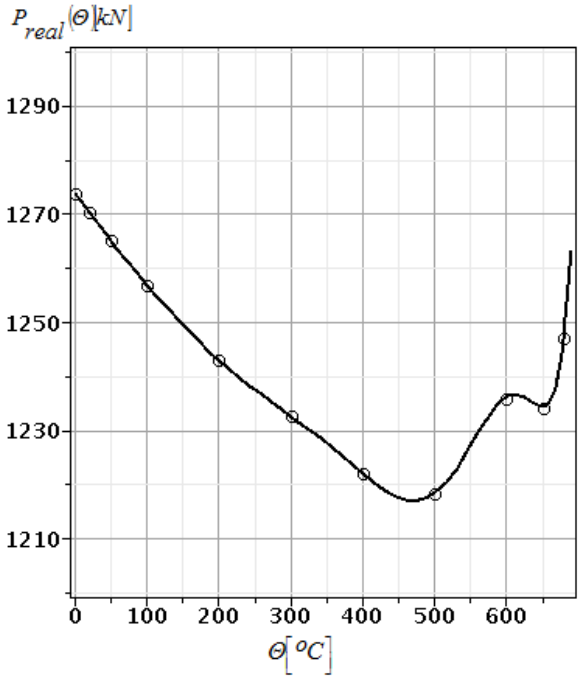

Fig.19. The response function $P_{real} = P_{real}(\theta)$.

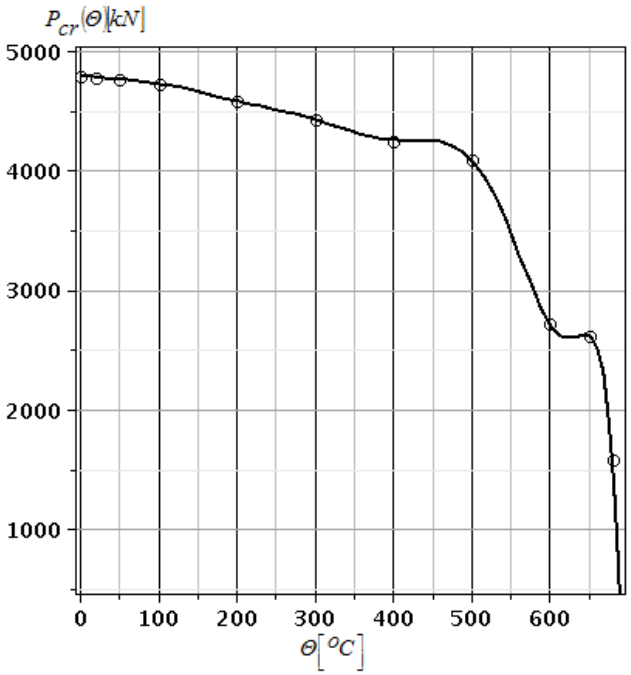

Fig.20. The response function $P_{cr} = P_{cr}(\theta)$.

Further, these polynomial functions have been processed in the computer algebra system MAPLE to obtain the first four probabilistic characteristics of the critical force as a function of the random input coefficient of variation. So that the expected values (Fig.21), the variances (Fig.22), skewness (Fig.23) and kurtosis (Fig.25) are computed at the temperature $\Theta=100^oC$ by the use of the even order stochastic perturbation theories from the second up to the twelfth one. Additionally, we attach the skewness (Fig.24) and kurtosis (Fig.25) for a higher temperature, i.e. $\Theta=500^oC$ to detect its influence on the probabilistic convergence of this method. Generally, it is seen that all the aforementioned characteristics obtained according to higher order stochastic perturbation techniques exhibit very similar results within these orders, while lower order techniques like the second and the fourth one should be completely disregarded. Interestingly, this remains true at $\Theta=100^oC$ for the enormously wide range on the input uncertainty $\alpha \in [0.0, 0.20]$.

The expected values despite of the particular perturbation order slightly decrease together with the input coefficient α (Fig.21), the variances increase in the same context also in a monotonous way (Fig.22). Further, we notice that skewness decreases through the negative values starting from initial *0* corresponding to a deterministic situation (Figs 23-24), whereas kurtosis increases being positive everywhere (Figs 25-26). Higher order characteristics exhibit the same general tendencies in lower and higher temperatures but their final fluctuations are more rapid. Very typically for the stochastic perturbation techniques, probabilistic characteristics computed according to different order theories diverge for an increasing value of the parameter α; sometimes rapid fluctuations of these statistics make this effect invisible (like in Figs 24-26). Finally, one needs to notice that both skewness and kurtosis differ from *0* elsewhere except a trivial deterministic case $\alpha=0$, which means the Gaussian temperature of the fire induces apparently non-Gaussian response in the context of the critical force. Therefore, the Cornel FORM reliability index has rather a limited significance and should be further replaced with the theory including non-symmetric and leptokurtic distributions of the stability limit state. It was the reason to study in detail the first two probabilistic moments inserted in this index at different temperatures corresponding to the heating by fire.

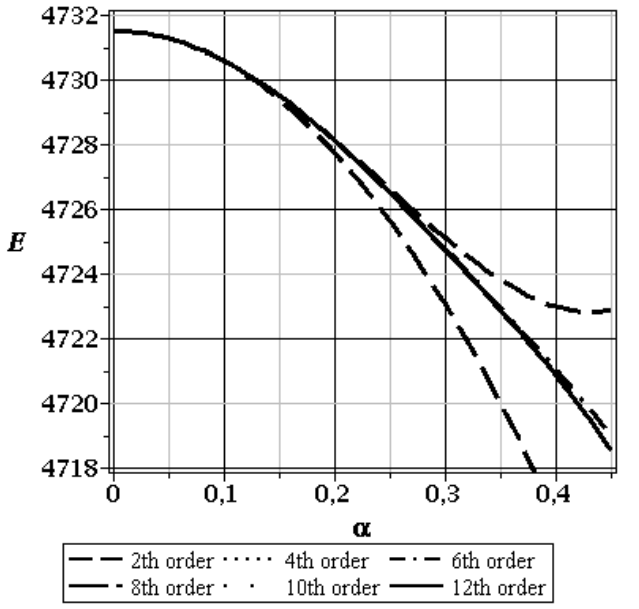

Fig.21. Expected value $E[P_{cr}]$, $\mathrm{E}[\Theta]=100^oC$.

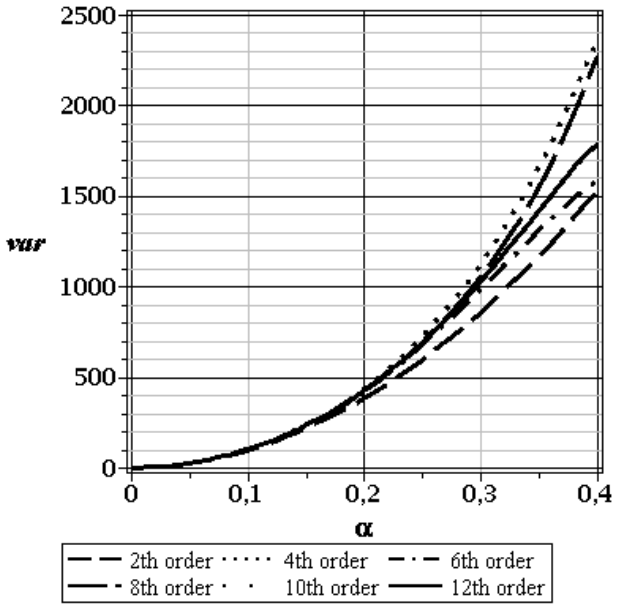

Fig.22. Variance $Var(P_{cr})$, $\mathrm{E}[\Theta]=100^oC$.

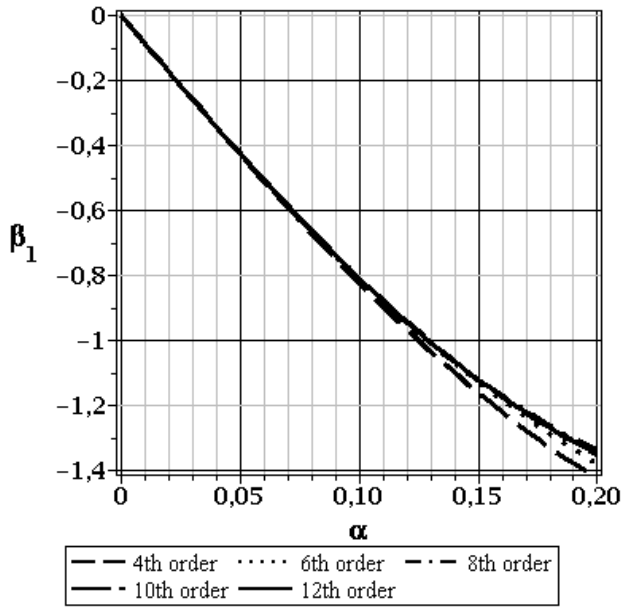

Fig.23. Skewness $\beta_1\left(P_{cr}\right)$, a comparison of the perturbation method and MCS, $\mathrm{E}[\Theta]=100^{o}C$.

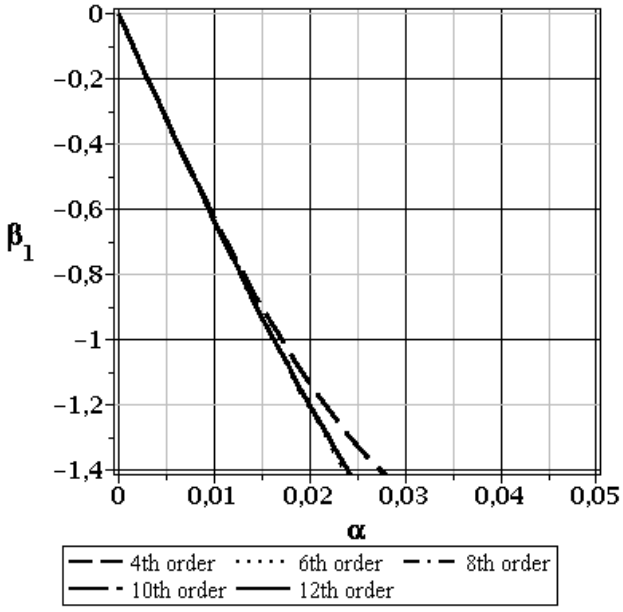

Fig.24. Skewness $\beta_1\left(P_{cr}\right)$, a comparison of the perturbation method and MCS, $\mathrm{E}[\Theta]=500^{o}C$.

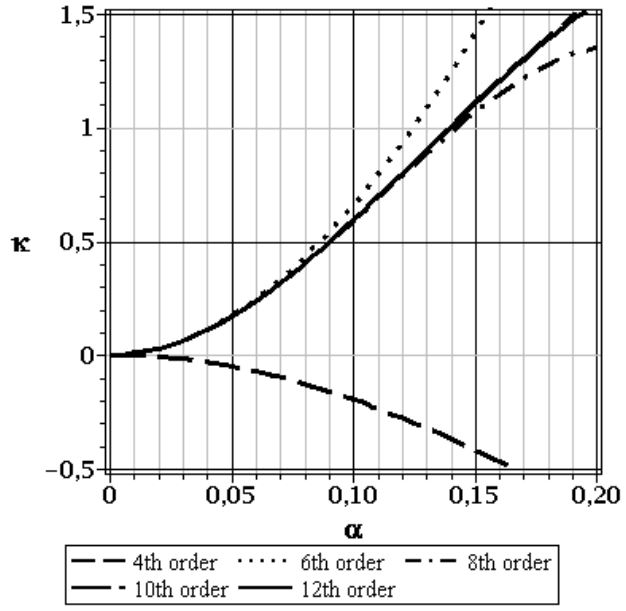

Fig.25. Kurtosis $\kappa\left(P_{cr}\right)$, a comparison of the perturbation method and MCS, $\mathrm{E}[\Theta]=100^{o}C$.

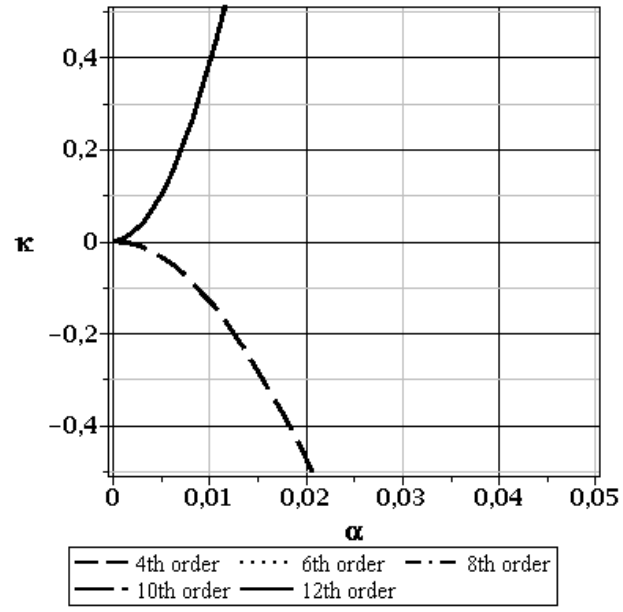

Fig.26. Kurtosis $\kappa\left(P_{cr}\right)$, a comparison of the perturbation method and MCS, $\mathrm{E}[\Theta]=500^{o}C$.

We collect for this purpose in pairs the expectations (Figs 27, 29, 31 and 33) and standard deviations (Figs 28, 30, 32 and 34) for the temperatures $300^{o}C$, $500^{o}C$, $600^{o}C$ and $680^{o}C$. A verification range of the input coefficient of variation has been decreased together with an increase of the fire temperature – from $\alpha=0.25$ at $\Theta=300^{o}C$ down to even $\alpha=0.10$ at the highest one $\Theta=680^{o}C$. The fundamental reason is an

apparent divergence of even the first two probabilistic moments computed for various perturbation orders. Reliable results are obtained right now with the use of the eight, tenth and twelfth Taylor expansion orders only. The input uncertainty has an increasing influence on these moments – the expected values for $\Theta=300^oC$ are almost insensitive (as far as the vertical axis range in Fig.27 is taken into account). They are more sensitive for $\Theta=500^oC$ (Fig.29) and suddenly after reaching $\Theta=600^oC$ may reach 0 (for $\alpha=0.11$ at $\Theta=600^oC$ and for $\alpha\cong 0.03$ at $\theta=680^oC$). Therefore, the stochastic method presented can detect the stability limit of the given structure in a presence of the Gaussian uncertainty in the fire temperature.

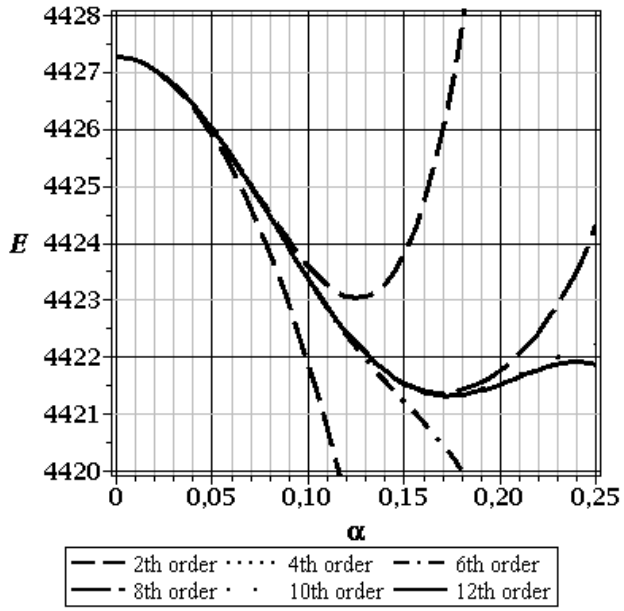

Fig.27. Expected value $E\left[P_{cr}\right]$, $\mathrm{E}[\Theta]=300^oC$.

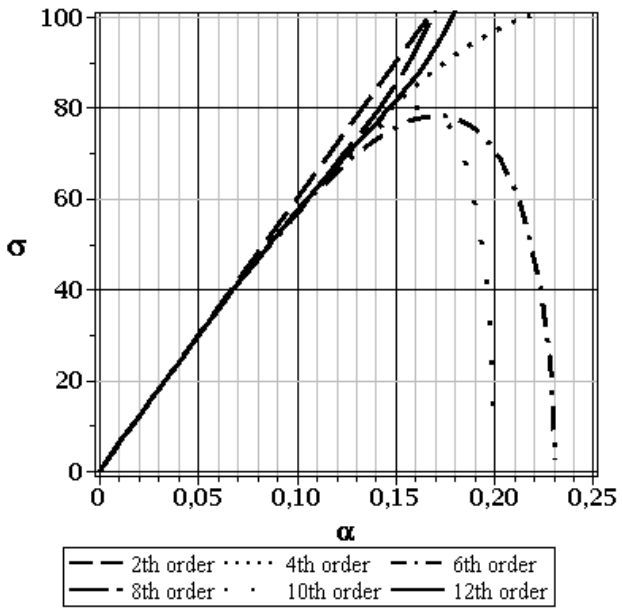

Fig.28. Standard deviation $\sigma\left(P_{cr}\right)$, $\mathrm{E}[\Theta]=300^oC$.

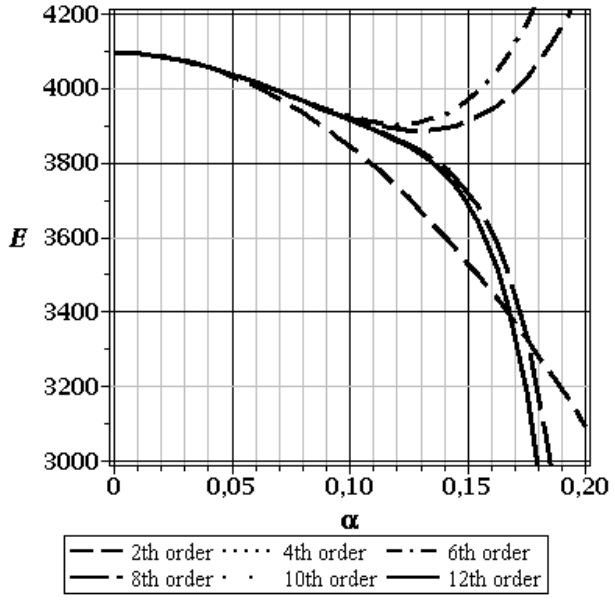

Fig.29. Expected value $E\left[P_{cr}\right]$, $\mathrm{E}[\Theta]=500^oC$.

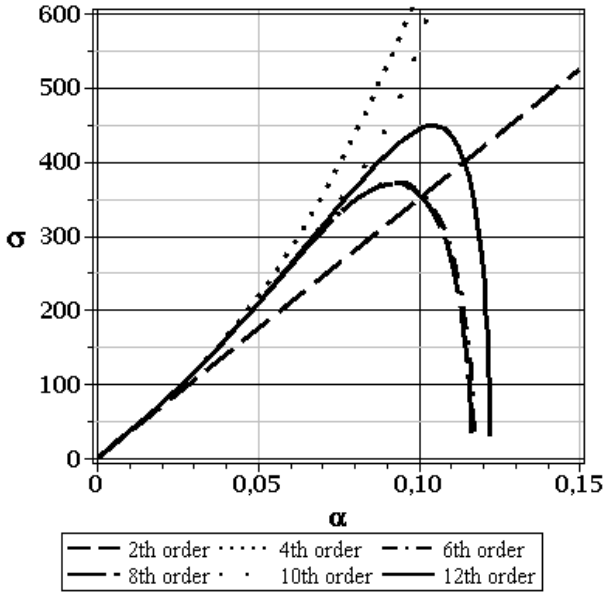

Fig.30. Standard deviation $\sigma\left(P_{cr}\right)$, $\mathrm{E}[\Theta]=500^oC$.

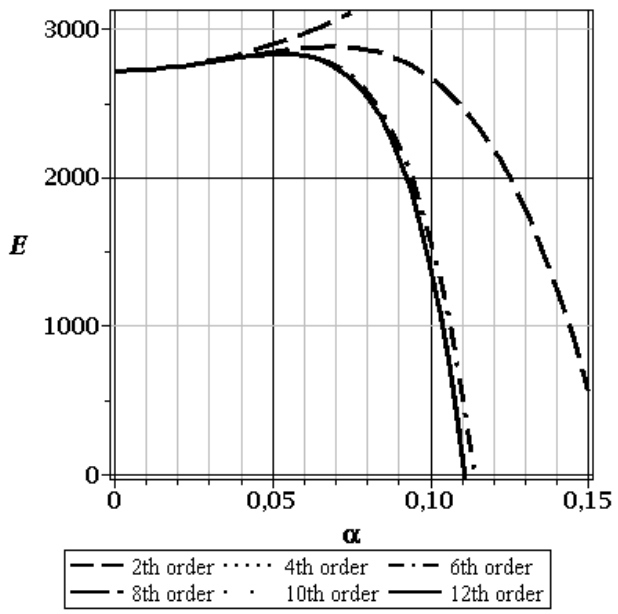

Fig.31. Expected value $E\lfloor P_{cr} \rfloor$, $\mathrm{E}[\Theta]=600^{o}C$.

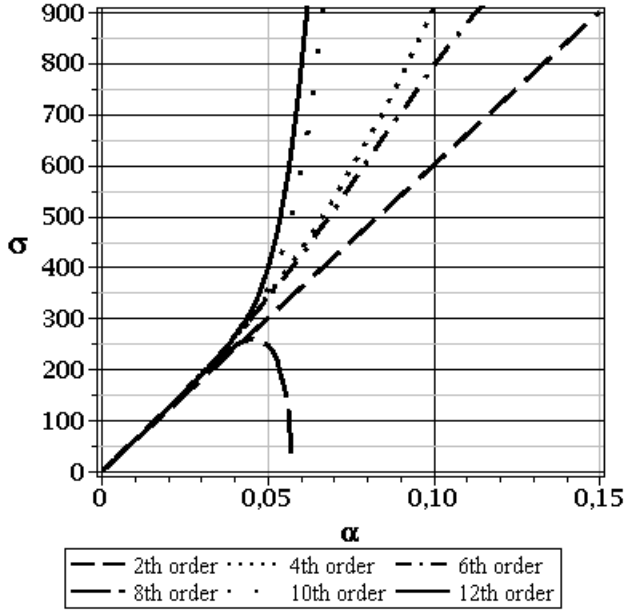

Fig.32. Standard deviation $\sigma\left(P_{cr}\right)$, $\mathrm{E}[\Theta]=600^{o}C$.

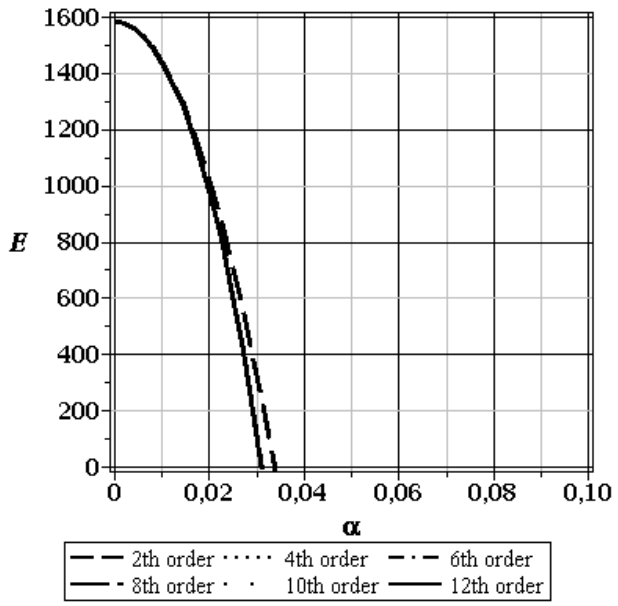

Fig.33. Expected value $E\lfloor P_{cr} \rfloor$, $\mathrm{E}[\Theta]=680^{o}C$.

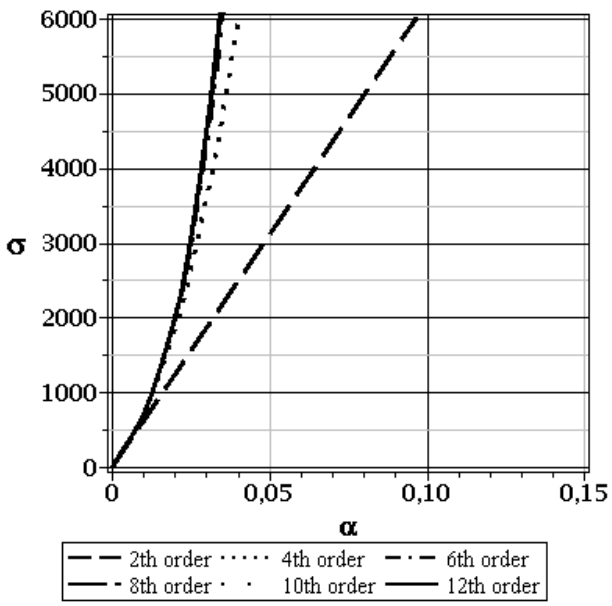

Fig.34. Standard deviation $\sigma\left(P_{cr}\right)$, $\mathrm{E}[\Theta]=680^{o}C$.

The negative expectations are of course completely disregarded since the physical interpretation of the sign change in the stability analysis. Standard deviations given in Figs 28, 30, 32 and 34 undergo even more dramatic fluctuations together with a fire temperature. They start from almost linear dependence upon the input coefficient α at $\Theta=300^{o}C$ (the same as before at $\Theta=100^{o}C$), then become highly nonlinear at $\Theta=500^{o}C$ for $\alpha \geq 0.10$ to decrease to *0* for $\alpha = 0.12$, which disqualifies the resulting reliability index for all

$\alpha > 0.12$. Above this temperature, see Figs 32 and 34 they still increase together with this parameter α but their extreme values are comparable to the corresponding expectation (at $\Theta=600^oC$) and even with a few times larger when compared to the corresponding expectation for $\Theta=680^oC$. All these observations and consequences look quite unusual when compared with many previous applications of the generalized higher order stochastic perturbation technique and its implementation as the SFEM.

Starting from probabilistic characteristics collected above (expected values, variances, kurtosis and skewness) one may analyze the reliability of the structure similarly to the first numerical example. The reliability index calculated according to the FORM approach has been presented in Tab.5. Analogously to the case studies with material uncertainty with no reduction of the additional parameters mean values with the temperature (Kamiński [2]) it is seen that as the variance of the critical force decreases together with an increase of the temperature, the FORM reliability index decreases. The expected values of this critical force magnitude decrease while increasing the input coefficient of variation, nevertheless an influence of the second order moment is decisive in this particular case. Generally, this observation reflects an engineering observation that steel structures lose their strength together with progressing fire exposure. Fire heating of this building must result in a failure and this is noticed at $\Theta=600^oC$ when this index reaches *0*. Summarizing, it should be emphasized that an important advantage of the method is the ability to analyze individual probabilistic characteristics as a function of the coefficient of variation, which offers undoubtedly the very significant acceleration of structural computations when compared to the traditional alternative - the Monte-Carlo simulation. One needs to notice that the output probability distribution is not strictly Gaussian, therefore an application of the Cornell theory is not very exact and should be replaced with a formula taking into account higher order statistics also.

Tab.5. Reliability index by the SFEM for $\mathrm{E}\left[\Theta = 500^{O}C\right]$ and $\mathrm{E}\left[\Theta = 600^{O}C\right]$.

	$\mathrm{E}\left[\Theta = 500^{O}C\right]$			$\mathrm{E}\left[\Theta = 600^{O}C\right]$		
α	$E[P_{cr}]$	$\mathrm{var}[P_{cr}]$	β	$E[P_{cr}]$	$\mathrm{var}[P_{cr}]$	β
0.02	*4084.40*	*7101.69*	*34.01*	*2745.63*	*11244.554*	*14.24*
0.04	*4054.63*	*32094.45*	*15.83*	*2802.00*	*56051.525*	*6.62*
0.06	*4010.78*	*80344.49*	*9.85*	*2814.97*	*359163.164*	*2.64*
0.08	*3960.16*	*153867.92*	*6.98*	*2595.96*	*5101506.682*	*0.60*
0.10	*3909.07*	*296257.70*	*4.94*	*1733.46*	*49240800.711*	*0.07*

5. Concluding remarks

The numerical analysis carried out in this work shows with no doubt that the steel structures are highly sensitive to high temperatures during fire accidents not only in the deterministic analysis but also in the stochastic context. The computational analysis provided in this paper shows that stochastic linearized buckling modeled with the help of the stochastic perturbation-based Finite Element Method program may be relatively easily implemented with interoperability of the computer algebra program and some classical Finite Element Method system. It is demonstrated here that a validity range of the tenth order stochastic perturbation method implemented as the SFEM and applied to determine the reliability index by the FORM highly depends on the input temperature of the element – for $\Theta\leq 600^oC$ input uncertainty $\alpha\in[0.00, 0.10]$ gives very accurate results, while $\Theta\geq 600^oC$ admits $\alpha\in[0.00, 0.05]$ only. Further, it is seen that the proposed Response Function Method yields quite reliable analytical approximations of the explicit interrelations in-between material structural design parameters and both discrete state parameters like displacements as well as global state functions like the critical load. It should be emphasized that the stochastic perturbation method is the first reliable method allowing a non-statistical determination of higher order probabilistic

moments and the resulting probability distribution. It is possible in particular to determine central moments of the higher order, kurtosis and skewness for the resulting critical load as the additional functions of the structural element mean temperature. Numerical analyses show here that a sufficiently good approximation is to engage the tenth order perturbation method, whose value usually is only slightly different from the next, twelfth consecutive perturbations. Noteworthy is the fact that the results obtained in the form of the reliability index can be directly expressed as a function of the input parameter uncertainty level, so that one can calculate even probabilistic entropy fluctuations. It remains evident after this study that the values of the reliability index concerning both Ultimate and Serviceability Limit States included into Eurocode design rules cannot be directly applied to the fire situation, where they should have significantly larger limit values. The stochastic perturbation method adopted for the analysis of buckling phenomena gives much larger capabilities for modeling reliability than other numerical methods. Reliability assessment using the higher order stochastic perturbation method related to stability of the selected steel structures has proven that quite good efficiency has been obtained using the method decisively less time-consuming than the Monte-Carlo simulation.

Nomenclature

b – input Gaussian random parameter
b^0 – mean value of the input Gaussian random parameter
$D_k(\theta)$ – temperature-dependent coefficients of polynomial expansion of the critical force with respect to random input b
$D_{[i]}(P_{cr})$ – ith partial derivative of the critical force with respect to random b
$D_{[i,j]}(P_{cr})$ – a product of ith and jth partial derivatives of the critical force with respect to random b
$E(\theta)$ – temperature-dependent Young modulus of the steel
$E[b]$ – expected value of the parameter b
$e_i(\theta)$ – temperature-dependent residuals in the Least Squares Method approximation
f_p – proportionality limit of the steel
f_y – plastic limit of the steel
g – limit function
$\boldsymbol{K}_{(\alpha)}^{(\sigma)}\left(\hat{F}_{(\alpha)};\theta\right)$ – temperature-dependent geometric stiffness matrix
$\boldsymbol{K}_{(\alpha)}^{(s)}(\theta)$ – temperature-dependent stiffness matrix
$k_E(\theta)$ – temperature-dependent for the Young modulus of the steel
$k_p(\theta)$ – temperature-dependent reduction factor of the proportionality limit for the steel
$k_y(\theta)$ – temperature-dependent reduction factor for the plastic limit of the steel
M – total number of discrete points in the Least Squares Method approximation
m – an order of polynomial representation for the critical load versus random input variable b
N – total number of random trials for Monte-Carlo simulations
n – random Taylor expansion order
P_{cr} – critical force
P_f – probability of survival of the given structure
$\boldsymbol{P}_{(\alpha)}(\theta)$ – deformation-independent component of the external load vector
$p_b(x)$ – probability density function of the parameter b
$\boldsymbol{Q}_{(\alpha)}(\theta)$ – deformation-dependent component of the external load vector
$\boldsymbol{R}_{(\alpha)}(\theta)$ – temperature-dependent external load vector
$\boldsymbol{r}_{(\alpha)}(\theta)$ – temperature-dependent structural displacement vector
$\mathrm{Var}(b)$ – variance of the parameter b

$v_{(\alpha)}(\theta)$ – temperature-dependent critical deformation of the structure
$\alpha(b)$ – coefficient of variation of random parameter b
α_T – coefficient of thermal expansion of the steel
β – reliability index
$\beta_1(b)$ – skewness of random parameter b
Δb – variation of the parameter b about its mean value b^0
$\Delta\theta$ – temperature fluctuation of the given structural element
ε – perturbation parameter
Φ – probability density function of the standardized Gaussian distribution
$\kappa(b)$ – kurtosis of random parameter b
$\lambda_{cr}(\theta)$ – temperature-dependent critical load multiplier
$\mu_k(b)$ – kth central probabilistic moment of random variable b
θ, Θ – given and structural element temperatures

References

[1] Elishakoff I. (1983): *Probabilistic Methods in the Theory of Structures*. – Wiley.

[2] Kamiński M. (2013): *The Stochastic Perturbation Method for Computational Mechanics*. – Chichester: Wiley.

[3] Waarts P.H. and Vrouwenvelder A.C.W.M. (1999): *Stochastic finite element analysis of steel structures*. – Journal of Constructional Steel Research, vol.52, pp.21-32.

[4] Ellobody E. (2011): *Interaction of buckling modes in castellated steel beams*. – Journal of Constructional Steel Research, vol.67, pp.814–825.

[5] Graham L.L. and Siragy E.F. (2001): *Stochastic finite-element analysis for elastic buckling of stiffened panels*. – Journal of Engineering Mechanics, vol.127, pp.91-97.

[6] Sadovský Z. and Drdácký M. (2001): *Buckling of plate strip subjected to localized corrosion – A stochastic model*. – Journal of Thin-Walled Structures, vol.39, pp.247-259.

[7] Papadopoulos V., Stefanou G. and Papadrakakis M. (2009): *Buckling analysis of imperfect shells with stochastic non-Gaussian material and thickness properties*. – International Journal of Solids and Structures, vol.46, pp.2800-2808.

[8] Steinböck A., Jia X., Höfinger G., Rubin H. and Mang H.A. (2008): *Remarkable postbuckling paths analyzed by means of the consistently linearized eigenproblem*. – International Journal for Numerical Methods in Engineering, vol.76, pp.156-182.

[9] Kalos M.H. and Whitlock P.A. (1986): *Monte Carlo Methods*. – New York: Wiley.

[10] PN-EN 1993-1-2:2005 *Eurocode 3: Design of steel structures - Part 1*-2: *General rules*. *Structural fire design.*

[11] Kleiber M. and Hien T.D. (1992): *The Stochastic Finite Element Method*. – Chichester: Wiley.

[12] Elishakoff I. (2000): *Uncertain buckling: its past, present and future*. – International Journal of Solids and Structures, vol.37, pp.6869-6889.

[13] Øksendal B. (2003): *Stochastic Differential Equations*. – Berlin-Heidelberg: Springer, 6th edition.

[14] Kamiński M. and Świta P. (2011): *Generalized Stochastic Finite Element Method in elastic stability problems*. – Computers and Structures, vol.89, pp.1241-1252.

[15] Cornell C.A. (1969): *A First-Order Reliability Theory for Structural Design. Study 3. Structural Reliability and Codified Design*. – Ontario: University of Waterloo.

[16] Bathe K.J. (1996): *Finite Element Procedures*. – Prentice Hall, Englewood Cliffs.

[17] Zienkiewicz O.C. and Taylor R.L. (2005): *The Finite Element Method for Solid and Structural Mechanics*. – 6th ed.. Elsevier, Butterworth–Heinemann, Amsterdam.

[18] Kamiński M. and Świta P (2011): *Reliability modeling in some elastic stability problems via the Generalized Stochastic Finite Element Method*. – Archives of Civil Engineering, vol.57, No.3, pp.275-295.

[19] Bendat J.S. and Piersol A.G. (1971): *Random Data: Analysis and Measurement Procedures*. – New York: Wiley.

Received: April 2, 2016

Revised: April 12, 2016